DEPOSITION OF POLYPYRROLE ON POROUS ALUMINIUM OXIDE

Kirill L. Levine,[A] Dennis E. Tallman[A, B] and Gordon P. Bierwagen[B]

[A] Department of Chemistry and [B] Department of Coatings and Polymeric Materials, North Dakota State University, Fargo, ND 58105-5516

We report the successful attempt of electrodeposition of polypyrrole (PPy) on the electrochemically developed porous oxide surface of aluminium alloy. Corrosion protection properties were assessed by potentiodynamic measurements and electrochemical impedance spectroscopy. It is shown that PPy on porous oxide significantly increases the corrosion potential making the surface more noble.

INTRODUCTION

Aluminium (Al) alloys, such as Al 2024-T3, are extensively used in the aircraft industry because of their light weight and excellent mechanical properties. Chemically pure Al is naturally protected from corrosion by an oxide layer. In the case of alloys this layer contains intermetallic impurities capable of causing galvanic corrosion. Corrosion of Al alloys is a serious industrial problem that typically is remedied by using hexavalent chromium (Cr^{6+}) coatings. Cr^{6+} coatings are a hazard for human health and the environment and due to new *OSHA* requirements these coatings have to be replaced. A possible alternative to Cr^{6+} coatings is conjugated polymer (CP) coatings that have shown to provide a very good corrosion protection on Al. Our research group has been exploring various conjugated polymers (e.g., polyaniline, polypyrrole and polythiophene) for use as corrosion control coatings, particularly for aluminum alloys [1-6]. Depositing a CP on Al alloy is a challenge because of a simultaneous growth of oxide layer. We have used an approach based on electron transfer mediators (ETMs) [1, 2] to deposit CPs on a surface of Al. In a recent publication we reported the influence of ETMs on the deposition of the CP polypyrrole (PPy) on Al alloy surface and have shown that depending on the type of substitution on benzene ring (carboxyl or sulfonate) and its position, mediating properties of the compound dramatically vary [7]. In this paper we report a successful approach for depositing PPy onto artificially grown Al oxide in the presence of electron transfer mediators, such as Tiron. The rationale for depositing PPy on the oxide layer is to combine the barrier properties of Al oxide with corrosion inhibiting properties of PPy. The Al oxide is a dielectric and in order to deposit CP onto oxide of a few microns thickness, it has to be porous. In this paper Al oxide was obtained electrochemically by a method that is usually used to obtain anodic porous alumina (APA), such as described in [8]. However, due to variations in the composition of the alloy[1], in our experiment the oxide was not comprised of regular distributed pores like in APA, but contained small pores of different size randomly distributed over the entire surface of the sample. Porous

[1]Composition of Al 2024-T3 (w/w %) is: 0.50 Si, 0.50 Fe, 3.8-4.9 Cu, 0.3-0.9 Mn, 1.2-1.8 Mg, 0.1 Cr, 0.25 Zn, 0.15 Ti, 0.15 other unspecified elements.

oxide (PO) was characterized by scanning electron microscopy (SEM), electrochemical impedance spectroscopy (EIS), and potentiodynamic (Tafel) experiments. Mechanical properties were assessed by nanoindent hardness and adhesion test. Composition of the PPy layer was characterized by Fourier transform infrared spectroscopy (FTIR).

EXPERIMENTAL

Materials

Pyrrole (Py) monomer and dihydroxybenzene disulfonate (DHBDS) (Tiron) were obtained from Aldrich Chemical Company; sodium sulfate was obtained from Alfa Aesar. All chemicals used were analytical grade. The Py was freshly distilled prior to use in nitrogen flow. The Al 2024-T3 panels were purchased from Q-Panel Co. and were prepared for electrodeposition by dry-polishing to 1500 grit with emery paper followed by rinsing with hexane. Solutions were prepared using Milli-Q water.

Methods

Galvanostatic Electrodeposition. An EG&G/PAR Model 273A potentiostat/galvanostat (Princeton Applied Research) was used for galvanostatic electrodeposition. The depositions were carried out in a one-compartment electrochemical cell at a current density of 1 mA/cm^2 for 2000 s. The working electrode was either bare Al 2024-T3 panel or panel with PO on it (12.5 cm^2). A platinum plate of equal area was used as the counter electrode and was arranged parallel to the working electrode. Electrodeposition was carried out in 1 M sodium sulfate electrolyte containing 0.1 M DHBDS and 0.1 M Py at pH 3. pH level was adjusted by addition of the appropriate amount of sulfuric acid.

Hardness testing. Hardness testing was performed on Buehler 5100 tester. 3 measurements were performed at loads 200, 300 and 500 g. Average of 3 measurements was taken to determine a point at every load. PPy deposition time for hardness testing was 500 s.

Fourier Transform Infrared Spectroscopy. A Magna-IR 850 Nicollet spectrometer was used to take FTIR spectra. The chamber with a sample was N_2 purged for 30 minutes prior to data acquisition. Each measurement consisted of 64 scans made at a resolution of 4 cm^{-1}. Ground powder of each studied sample was mixed with KBr and pressed into a pellet at 7000 psi, 30 s. OMNIC E.S.P. 5.1 software was used for data analysis.

Electrochemical Impedance Spectroscopy. The electrochemical cell for EIS consisted of a cylinder glass tube 7.5 cm long and 5 cm^2 in cross-section, filled with dilute Harrison solution (DHS) composed of 0.05 w/w % NaCl and 0.35 w/w % $(NH_4)_2SO_4$. The tube was attached to a sample by metal clip and rubber O- ring. The coated Al panel was used as the working electrode. The reference electrode was a SCE and the counter electrode was a platinized grid. During the experiment the cell was shielded in a Faraday cage. Experiments were performed in a frequency range from 10^{-1} to 10^5 Hz using a 10 mV AC

perturbation. Gamry potentiostat ESA400, and Gamry Framework software were used to perform experiment and for data acquisition.

Potentiodynamic measurements. The electrochemical cell used for potentiodynamic measurements was as described above. ESA 400 potentiostat powered by Gamry Framework software was used to perform experiment.

Scanning Electron Microscopy. Scanning electron microscopy (SEM) was carried out on a JEOL JSM 6300 scanning electron microscope on Au sputtered samples at potential 15 kV.

Adhesion testing. The adhesion of electrodeposited coatings was measured using an Elcometer 106 Adhesion Tester. An epoxy resin (907 adhesive, Miller Stephenson Corporation) was used to attach a dolly to the coating and the specimen was allowed to cure overnight at room temperature. Before measurement, the samples were heated to 50 ºC for 1 h and then cooled to ambient temperature. For each PPy deposition time, measurements were made at two different locations on the panel and the average was taken.

RESULTS AND DISCUSSION

Structure and morphology

Electrochemical constant current deposition of PPy on PO surface required potentials that were sufficiently higher than usually observed during PPy deposition on bare Al alloy surface. The curve at the bottom of Figure 1 shows deposition of PPy onto Al alloy surface in the presence of DHBDS. In this case the deposition potential was 0.6-0.65 V vs. Ag/AgCl that is a typical value for the deposition in the presence of this mediator [7]. When the Al alloy was preliminary coated with PO, the deposition started at 5.2 V vs. Ag/AgCl, reaching appr. 7 V after the first 50 s of the experiment, followed by a slow decrease to 6.5 V. Without DHBDS deposition on the oxide surface was not possible (the deposition potential was above 8 V and although an electrode surface changed its, no PPy film formation was observed.) In the presence of DHBDS a smooth adherent coating was formed. However, it took longer time to obtain PPy film of given thickness on oxide, suggesting that on PO the current efficiency of PPy formation was less than 100%. Although PPy deposition on PO and on bare surface was carried out with a significant difference of applied potentials, the PPy structure on the both of these surfaces was FTIR identical (Figure 2). Major FTIR peaks characteristic for PPy were: 3130 cm^{-1} (N-H [9]), 1475 cm^{-1} (C-N stretching [10]), 1176 cm^{-1} (C-N stretching [11]), 1170 cm^{-1} (C-H in plane [12]), 1035 cm^{-1} (N-H and C-H in plane deformation [13]). Slight differences were found below 772 cm^{-1}, characteristic of C-H in ring vibrations that were shifted to lower wavenumbers. Similarity of PPy structures determined by FTIR suggests that in the presence of ETM the overpotential of PPy deposition was negligible and did not result in CP overoxidation, usually observed if the potential of PPy deposition is too high [14]. The applied potential (neglecting electrolyte resistance) can be represented as:

$$E_{appl}=I \cdot R_{ox} + E_{PPy\ dep} \qquad \text{Eq.1}$$

where E_{appl} is the applied potential, I the current, R_{ox} the resistance of the oxide to charge flow, and $E_{PPy\ dep}$ the potential required to PPy deposition. Although this expression seems to be a reasonable approximation when Tiron is used a mediator, it has to be used with caution since overpotential of PPy deposition in pores can differ from that at bare Al surface.

Assuming that $E_{PPy\ dep}$ is the same in the presence and absence of the oxide (600 mV) and subtracting it from the steady state potential of deposition on oxide (6500 mV), an oxide resistance R_{ox} can be estimated from Eq. 1 as $1.2 \cdot 10^2$ Ohm. From Eq. 2

$$R_{ox} = \rho \frac{l}{A} \qquad \text{Eq. 2}$$

where l is the oxide thickness (2.4 μm from interference measurements), A is sample area, volume resistivity of oxide (ρ) can be determined as $2.5 \cdot 10^7$ Ω·cm. The difference between this value and values typical for Al_2O_3 that is $>10^{14}$ Ω·cm is possibly due to pores. R_{ox} determined from Eq. 1 is by at least an order of magnitude less than that obtained by extrapolation to zero frequency of Real component of the Impedance from Bode plots. Such significant difference possibly arises from PPy film function as a secondary electrode in contact with PPy in pores that is a primary electrode during PPy electrodeposition.

The presence of an oxide at the surface was also confirmed from hardness testing summarized in Table 1. In crystalline form Al oxide (alumina) possess very high hardness. Bare Al surface coated with PO also shows increased hardness that decreases when a rather smooth PPy film appears on it. However, PPy on PO still appears to possess an increased hardness relative to PPy on bare Al due to cumulative effect of both oxide and PPy.

Table 1. Hardness testing of Al surface.

	Bare Al, ambient oxide	Aluminum with PO	PPy deposited on bare Al	Al with PO and PPy layer on it
Hardness, x100 Vickers	1.7	1.9	1.1	1.6

Adhesion testing has shown high values of adhesion of PPy to the surface of porous oxide (The oxide structure is clearly identified as porous by SEM (Figure 3 A and B) in contrast to bare Al (Figure 3 C and D). SEM image of PPy obtained on PO (Figure

4 A and B) shows dense and uniform PPy layer with PPy globules on the top of it. PPy globules on oxide look similar to ones on bare Al (Figure 4 C), but smaller in size.

Table 2) that did not vary significantly with the time of PPy deposition. High values of adhesion can be explained by mechanical interaction between PPy and Al oxide as shown in a scheme below.

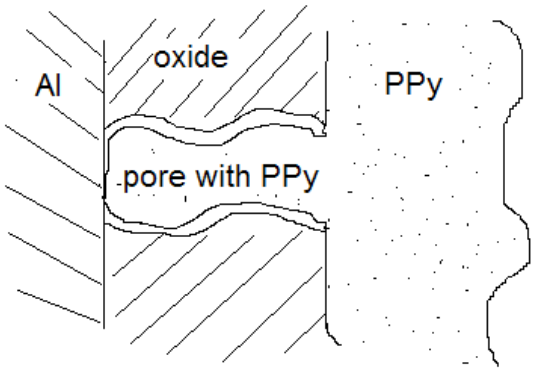

The oxide structure is clearly identified as porous by SEM (Figure 3 A and B) in contrast to bare Al (Figure 3 C and D). SEM image of PPy obtained on PO (Figure 4 A and B) shows dense and uniform PPy layer with PPy globules on the top of it. PPy globules on oxide look similar to ones on bare Al (Figure 4 C), but smaller in size.

Table 2. Adhesion testing. PPy deposition regimes: 0.1 M Py (freshly distilled), 0.1 N Tiron, 1 M Sodium Sulfate, pH3, 0.5 mA/cm^2 (on oxide), 1mA/cm^2 (on non-treated surface).

Type of sample	Adhesion, PSI	Type of failure
Bare Al control	400 - 750	cohesive
PPy on Al	50	Adhesive
PPy on oxide, 500 s deposition	700	Adhesive
PPy on oxide, 1000 s deposition	600	Adhesive
PPy on oxide, 2000 s deposition	500	Adhesive/Cohesive

The barrier properties of formed oxide layer were assessed by EIS measurements. Figure 5 shows impedance of coatings extracted from Bode plots at 0.1 Hz frequency. Initially high values of impedance decrease with time possibly because due to ingress of electrolyte into the porous oxide and /or attack of the oxide layer. Immediately after immersion in DHS, the impedance of oxidized surface was approximately 1 order of magnitude higher than that of the bare surface. After approximately one month of immersion in DHS, the difference in impedance was similar indicating that the oxide layer retained its barrier properties.

Potentiodynamic (Tafel) experiments (Figure 6) have shown higher corrosion potential of PPy on PO surface (-0.1 V vs. SCE[2]) than that of PPy on bare Al alloy panel (-0.45 V vs. SCE). The potential for Al with oxide but without PPy was determined to be (-0.3 V vs. SCE), significantly higher than that of bare Al (-0.9 V vs. SCE). The corrosion potential of a free standing PPy film measured as open circuit potential was found to be 0.02 – 0.05 V vs. SCE, close to value obtained for PPy on PO. Corrosion currents in passive region were much lover (by 1.5 – 2 orders) for PPy on PO and PO compared to PPy on bare Al and bare Al control.

CONCLUSIONS

In the presence of electron transfer mediator DHBDS, PPy coatings were successfully prepared on porous aluminium oxide surface. The coatings possessed high hardness, high adhesion to Al and have shown corrosion protection performance in potentiodynamic experiments. PPy on PO surface revealed an increased corrosion potential in DHS, therefore making the surface less vulnerable to galvanic corrosion. A higher impedance of oxide coated surface was revealed by EIS. Therefore, corrosion protection properties of PPy combined with the barrier properties of Al oxide, suggest an extra possibility for corrosion protection of active metals with CPs.

ACKNOWLEDGEMENTS

Authors would like to gratefully acknowledge Mr. Scott Payne and Mr. Damien Mathew for their performance with instrumentation, and Dr. Syed Ahmad from the Center for Nanoscale Science and Engineering for his contribution to hardness measurements. This work was supported by the Air Force Office of Scientific Research (grant no. FA9559-04-1-0368) and also by the United States Air Force Research Laboratory, University of Dayton (grant no. RSC02050).

REFERENCES

1. He, J.; Gelling, V. J.; Tallman, D. E.; Bierwagen, G. P.; Wallace, G. G., Conducting polymers and corrosion III. A scanning vibrating electrode study of poly(3-octyl pyrrole) on steel and aluminum. *Journal of the Electrochemical Society* **2000,** 147, (10), 3667-3672.
2. Tallman, D. E.; Pae, Y.; Bierwagen, G. P., Conducting polymers and corrosion: part 2 - polyaniline on aluminum alloys. *Corrosion (Houston)* **2000,** 56, (4), 401-410.
3. Tallman, D. E.; Spinks, G.; Dominis, A.; Wallace, G. G., Electroactive conducting polymers for corrosion control part 1. General introduction and a review of nonferrous metals. *Journal of Solid State Electrochemistry* **2002,** 6, (2), 73-84.

[2] Other potentials also vs. SCE.

4. He, J.; Tallman, D. E.; Bierwagen, G. P., Conjugated Polymers for Corrosion Control: Scanning Vibrating Electrode Studies of Polypyrrole-Aluminum Alloy Interactions. *Journal of the Electrochemical Society* **2004,** 151, (12), B644-B651.
5. Tallman, D. E.; He, J.; Gelling, V. J.; Bierwagen, G. P.; Wallace, G. G., Scanning vibrating electrode studies of electroactive conducting polymers on active metals. *ACS Symposium Series* **2003,** 843, (Electroactive Polymers for Corrosion Control), 228-253.
6. Gelling, V. J.; Wiest, M. M.; Tallman, D. E.; Bierwagen, G. P.; Wallace, G. G., Electroactive-conducting polymers for corrosion control 4. Studies of poly(3-octyl pyrrole) and poly(3-octadecyl pyrrole) on aluminum 2024-T3 alloy. *Progress in Organic Coatings* **2001,** 43, (1-3), 149-157.
7. Levine, K. L.; Tallman, D. E.; Bierwagen, G. P., The Mediated Electrodeposition of Polypyrrole on Aluminium Alloy. *Australian Journal of Chemistry* **2005,** 58, (4), 294-301.
8. Zhao, Y.; Chen, M.; Zhang, Y.; Xu, T.; Liu, W., A facile approach to formation of through-hole porous anodic aluminum oxide film. *Materials Letters* **2005,** 59, (1), 40-43.
9. Szymanski, H. A.; Erickson, R. E., *Infrared Band Handbook. 2nd ed*. 1970; p 1491 pp (2 vols).
10. Song, M.-K.; Kim, Y.-T.; Kim, B.-S.; Kim, J.; Char, K.; Rhee, H.-W., Synthesis and characterization of soluble polypyrrole doped with alkylbenzenesulfonic acids. *Synthetic Metals* **2004,** 141, (3), 315-319.
11. He, C.; Yang, C.; Li, Y., Chemical synthesis of coral-like nanowires and nanowire networks of conducting polypyrrole. *Synthetic Metals* **2003,** 139, (2), 539-545.
12. Chen, W.; Li, X.; Xue, G.; Wang, Z.; Zou, W., Magnetic and conducting particles: preparation of polypyrrole layer on Fe3O4 nanospheres. *Applied Surface Science* **2003,** 218, (1-4), 215-221.
13. Omastova, M.; Trchova, M.; Kovarova, J.; Stejskal, J., Synthesis and structural study of polypyrroles prepared in the presence of surfactants. *Synthetic Metals* **2003,** 138, (3), 447-455.
14. Rodriguez, I.; Scharifker, B. R.; Mostany, J., In situ FTIR study of redox and overoxidation processes in polypyrrole films. *Journal of Electroanalytical Chemistry* **2000,** 491, (1,2), 117-125.

FIGURES

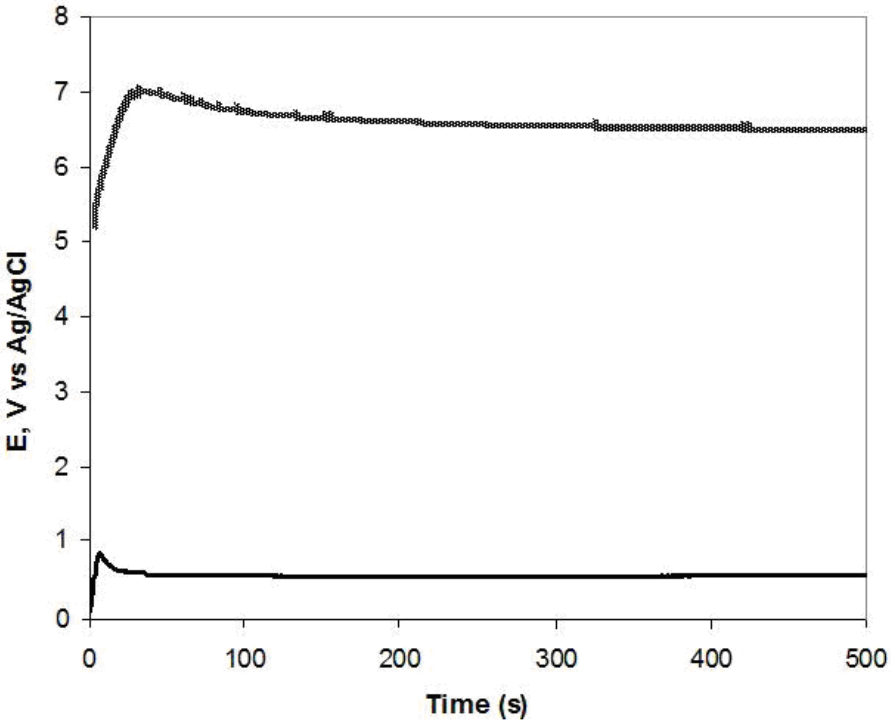

Figure 1. Galvanostatic deposition of PPy on the surface of aluminum alloy with oxide (top) and without oxide layer (bottom).

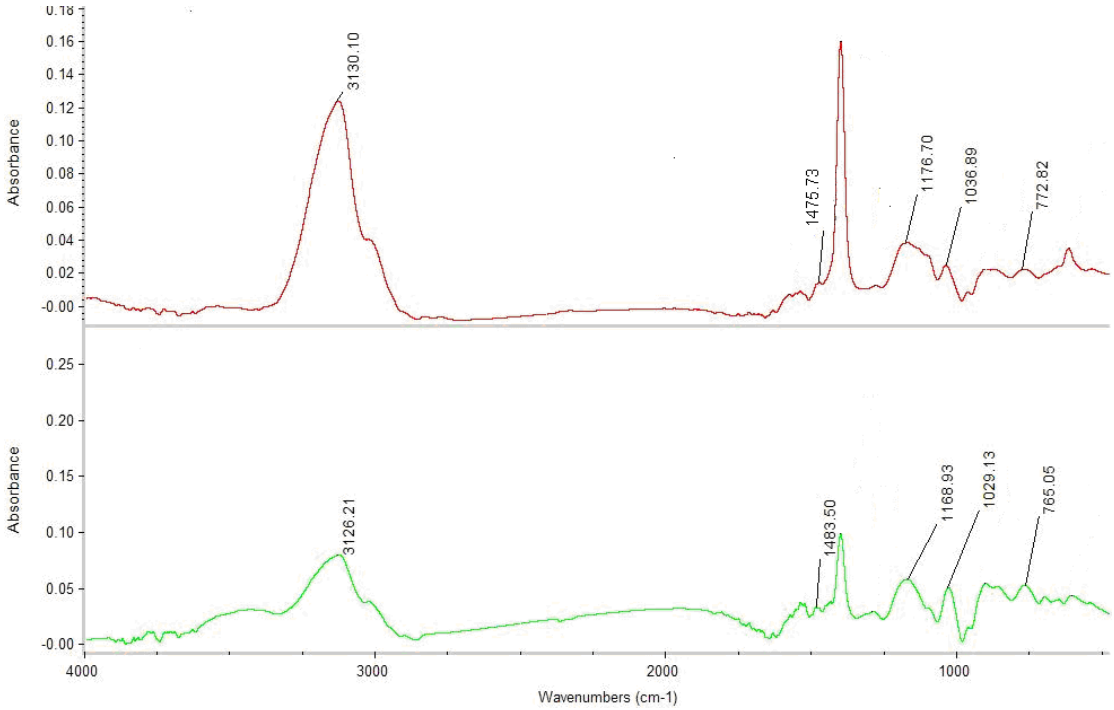

Figure 2. FTIR spectra of PPy. Upper spectrum – obtained on untreated surface, bottom spectrum - on PO.

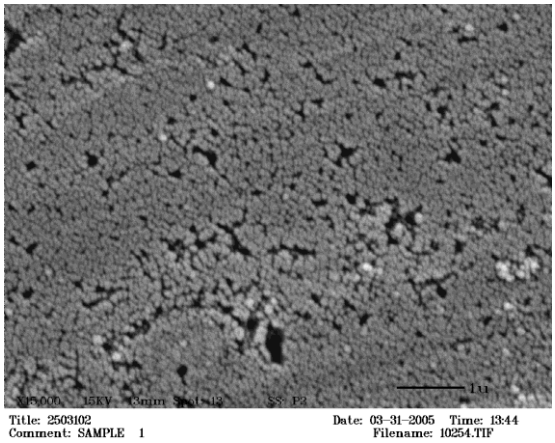

a

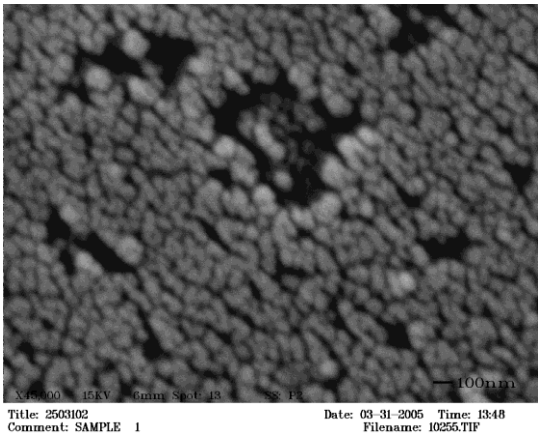

b

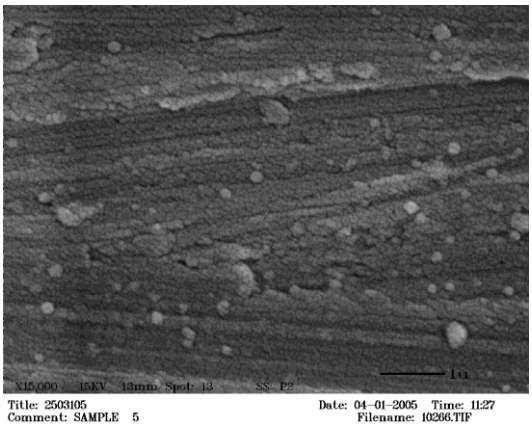

c

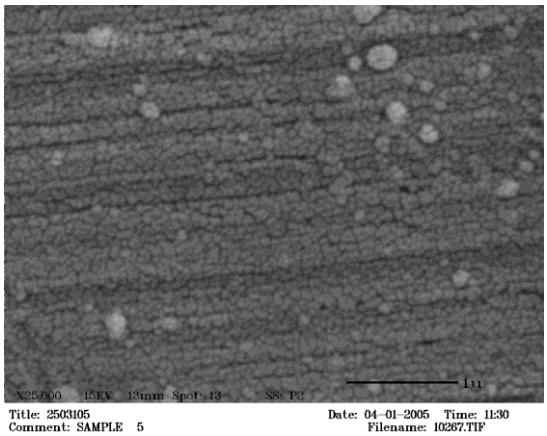

d

Figure 3. SEM images of PO aluminium (a and b) and regular aluminium surface (c and d).

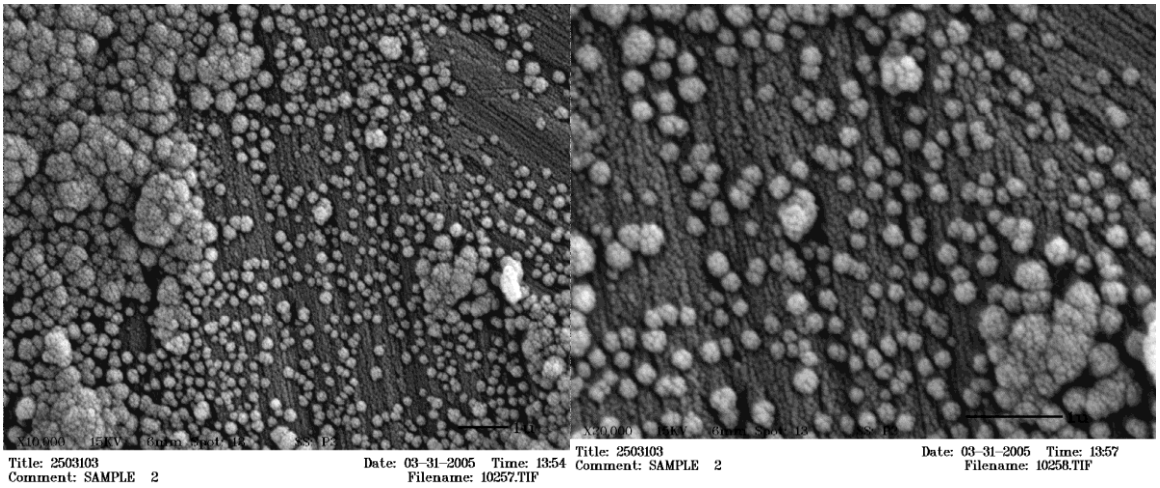

a b

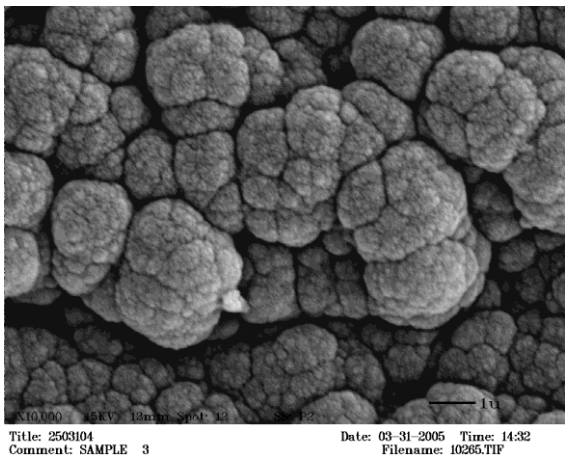

C

Figure 4. SEM images of PPy on PO aluminium (a and b), and (C) PPy on bare surface at magnification. [PPy deposition: 500 s, 1 mA/cm^2, 0.1 M Py, 1 M Na_2SO_4, pH3].

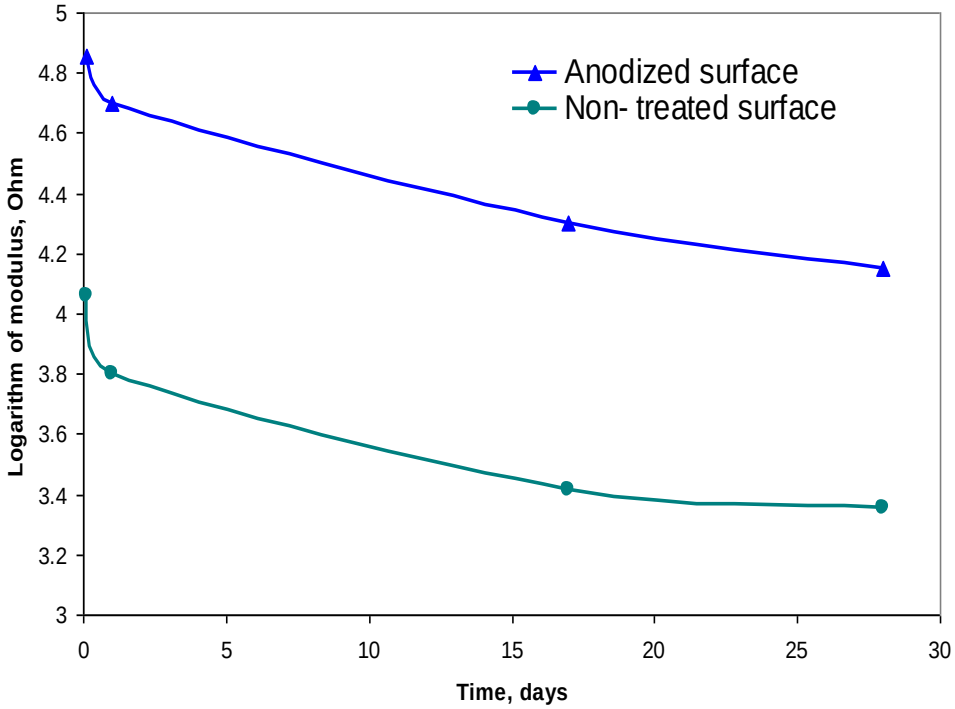

Figure 5. Logarithm of impedance of Al surface with PO as a function of time of immersion in DHS at frequency 0.1 Hz.

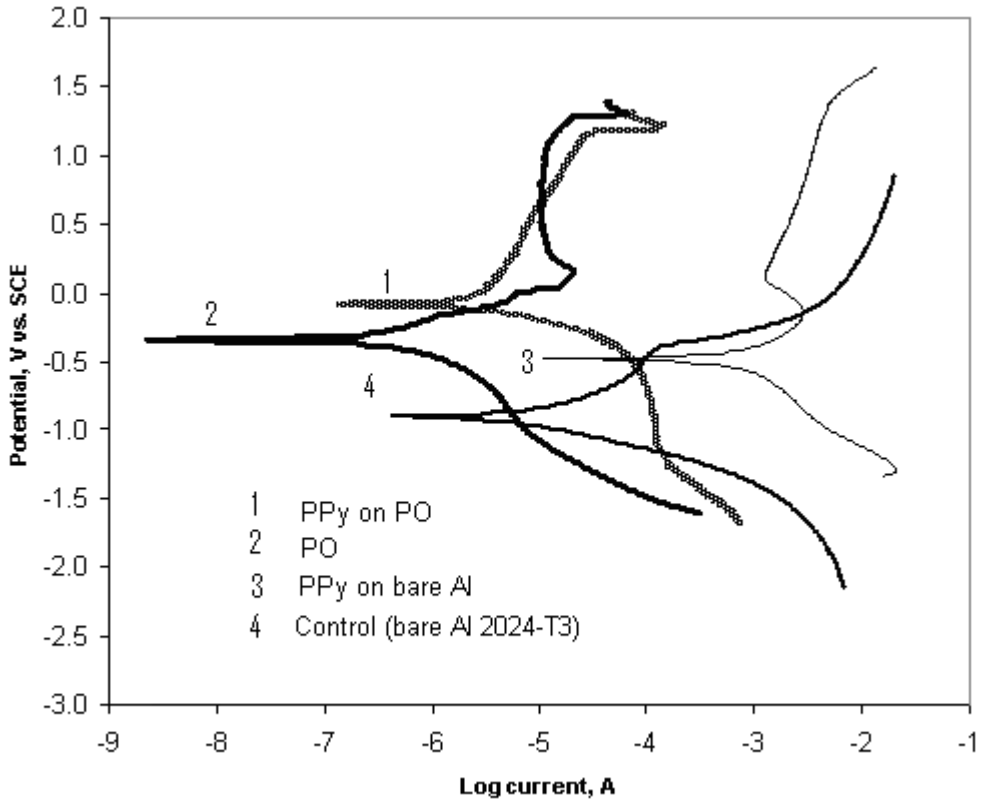

Figure 6. Potentiodynamic (Tafel) plots.

Key words: polypyrrole, aluminium alloy, corrosion protection, electron transfer mediation, Tiron